Hyperspherical approach to double-electron excitation of He by fast-ion impact

Kengo Moribayashi, Ken-ichi Hino, and Michio Matsuzawa
Department of Applied Physics and Chemistry, The University of Electro-Communications, 1-5-1 Chofu-ga-oka Chofu-shi, Tokyo 182, Japan

M. Kimura
Argonne National Laboratory, Argonne, Illinois 60439
and Department of Physics, Rice University, Houston, Texas 77251
(Received 24 June 1991; revised manuscript received 13 August 1991)

Double-electron-excitation processes of He atoms by proton, antiproton, and C^{6+}-ion impact have been theoretically investigated using the second-order Born approximation and the close-coupling method in the energy regime of MeV/u. The semiclassical impact-parameter method with a straight-line-trajectory approximation is employed to describe the collision processes. Hyperspherical wave functions are adopted to take full account of the strongly correlated motion of two atomic electrons in He. For proton and antiproton impact, it is found that the first-order mechanism dominates for excitation to the $(2s2p)\,^1P^o$ excited state, while the second-order processes play a significant role in excitation to the $(2s2s)\,^1S^e$, $(2p2p)\,^1S^e$, and $(2p2p)\,^1D^e$ excited states at a few MeV/u. It should be noted that the doubly excited $(2s2p)\,^1P^o$ state plays an important role as an intermediate state in these second-order processes in addition to the singly excited $1s2p\,^1P^o$ state. It is also found that the difference for the double-electron-excitation processes by proton impact and by antiproton impact is much smaller than that for the double-ionization processes in this energy range. For the C^{6+}ion impact, higher-order mechanisms play more important roles at a few MeV/u. The excitation mechanism is also discussed based on the classification scheme of the correlation quantum numbers, which enables us to obtain a more direct physical insight into the collision mechanism.

PACS number(s): 34.50.Fa, 31.50.+w, 31.20.Tz

I. INTRODUCTION

Recently much research has been done to understand the mechanism of electron correlation experimentally and theoretically. In studying the role of electron correlation in ion-atom collisions, there are several interesting phenomena such as double excitation, double ionization, double charge transfer, transfer excitation, and so forth. In 1986, Andersen *et al.* carried out an experiment at CERN on double ionization of He atoms at a few MeV/u impact energy by proton and antiproton impact [1]. In their experiment, it has been found that the cross section by the antiproton impact is about two times as large as that by the proton impact in spite of the high impact energy used, while both single-ionization cross sections are almost equal to one another. There have been several theoretical attempts to explain the difference between the two sets of double-ionization cross sections [2–6]. Recent studies on double ionization [2,3] have suggested the importance of electron correlation. However, it is rather difficult to treat double ionization theoretically. Therefore it is quite interesting to investigate the double excitation process

$$A^{Z_p+}+\mathrm{He}(1s^2)\rightarrow A^{Z_p+}+\mathrm{He}^{**}(2l2l') \qquad (1)$$

because this collision process is the simplest one in which the correlation effect is expected to play a decisive role. Here A^{Z_p+}

There have been some experimental and theoretical studies on process (1). Giese *et al.* [7] and Pedersen and Hvelplund [8] investigated these processes experimentally. Giese *et al.* used e^-, proton, $C^{q+}(q=4-6)$, and $F^{q+}(q=7-9)$ as projectile, and measured the sets of the cross sections from the ground state to the three doubly excited states $(2s2s\,^1S^e$, $2s2p\,^1P^o$, $2p2p\,^1D^e)$ at 1.5 MeV/u impact energy. On the other hand, Pedersen and Hvelplund measured the cross sections to the $(2p2p\,^1D^e+2s2p\,^1P^o)$ state at 1.84 MeV/u impact energy by e^-, proton, and $C^{q+}(q=4-6)$ ion impact. They could not resolve the $2p2p\,^1D^e$ state from the $2s2p\,^1P^o$ state. Fritsch and Lin [9] made theoretical studies on process (1), using the close-coupling method with the He wave functions based on the configuration-interaction method.

So far, Matsuzawa and co-workers [11–14] have been investigating collisional properties of He atoms in strongly correlated high-lying doubly excited states, i.e., how the He atoms in the correlated doubly excited states behave when they interact with charged particles perturbatively. These studies indicate that the He atoms in strongly correlated doubly excited states tend to conserve their internal states as a flexible "e-He^{2+}-e" triatomic molecule during the excitation processes except for the restriction arising from the Pauli exclusion principle. Namely, these simple propensity rules mainly apply to first-order processes. However, in actual collision processes, second- and higher-order processes may become

important particularly for the optically forbidden transitions. It is interesting and essential to investigate theoretically the simplest two-electron collision processes such as process (1) in order to understand the correlation mechanism in collision dynamics.

The purpose of the present paper is to understand the role of the correlation effects in the simplest collision process, i.e., the double excitation process of He by fast-ion impact such as the proton, antiproton, and C^{6+} ion, in which the electron-electron correlation is expected to play an essential role. We expand the total wave function in terms of the He wave functions whose origin is taken at the He^{2+} nucleus and generate the He wave functions by hyperspherical-coordinate method to take into account the electron-electron correlation effects. We calculate the double-electron-excitation cross sections from the ground state to the four lowest doubly excited states using (i) the second-order-Born approximation and (ii) the close-coupling method, and discuss the mechanism of the double-electron excitation by comparing our calculated results with those of other experimental and theoretical studies.

II. THEORETICAL TREATMENT

A. Coupling with the continuum

All doubly excited states of He atoms are embedded and hence coupled with the continuum, and give rise to autoionization processes, that is,

$$He^{**} \rightarrow He^{+} + e^{-} . \tag{2}$$

If these lifetimes are comparable to or shorter than the collision ones, we must consider the continuous states explicitly, i.e., $He^{+}+e^{-}$, to calculate the cross sections from the ground state to doubly excited states. According to the calculations by Burke [15], the autoionzition widths of the $2s2s\ ^1S^e$, $2s2p\ ^1P^o$, $2p2p\ ^1S^e$, and $2p2p\ ^1D^e$ states are 0.002 59, 0.000 805, 0.000 345, and 0.001 35 a.u., respectively. As a result, these lifetimes are estimated to be longer than 300 a.u. On the other hand, in the incident energy region of projectiles, i.e., more than 1 MeV/u (the velocity of more than 5 a.u.), we estimate the collision time to be about 5 a.u. Therefore the autoionization lifetime is at least 60 times as long as the collision time. Hence, in this study, we have ignored the coupling with the continuum.

B. Method of calculation and the wave function employed

We neglect the charge transfer channels in process (1) because charge transfer cross sections are quite small in comparison with excitation cross sections in the high incident energies studied here. Therefore we expand the total wave function in terms of the He wave functions centered on the He^{2+} nucleus. We generate the He wave functions employing the hyperspherical-coordinate method. This allows us to describe the electron-electron correlation accurately. Table I lists the states included in the close-coupling calculation with the labelings based on the conventional independent particle model and gives the values of the binding energies calculated from our wave functions [16–18]. Our calculated energy levels reproduce those of the close-coupling method plus correlation [15] and those based on the complex rotation method using elaborate Hylleraas-type trial wave functions [19] within at most a few percent.

We calculate double-electron-excitation cross sections using two different treatments, namely, (i) the second-order Born approximation and (ii) the close-coupling method within a semiclassical impact-parameter formalism. For the description of the collision processes, we have to evaluate the following matrix elements of the interaction potential between the projectile and the atomic electrons:

$$V_{ij} = Z_p \left\langle j \left| \frac{1}{r_{p1}} + \frac{1}{r_{p2}} \right| i \right\rangle . \tag{3}$$

TABLE I. Doubly excited states included in the calculation of the cross sections and their binding energies. The first column gives a set of the quantum numbers for the main electronic configuration based on the independent particle model, the second column shows a set of correlation quantum numbers, the third column gives the values of the binding energies of the doubly excited states calculated from our hyperspherical wave functions, and columns (4)–(6) give the binding energies calculated by Fritsch and Lin [10], Burke [15], and Ho [19], respectively. The unit of energy is the Rydberg. The entries given in parentheses in columns (3) and (4) are the relative errors (%) for the energies calculated by Burke.

(1)	(2)	(3)	(4)	(5)	(6)
$1s1s\ ^1S^e$	$[1(0,0)^{+}1]\ ^1S^e$	−5.791	−5.754		
$1s2s\ ^1S^e$	$[1(0,0)^{+}2]\ ^1S^e$	−4.280	−4.278		
$1s2p\ ^1P^o$	$[1(0,0)^{o}2]\ ^1P^o$	−4.243	−4.244		
$2s2s\ ^1S^e$	$[2(1,0)^{+}2]\ ^1S^e$	−1.545(0.7)	−1.544(0.8)	−1.556	−1.556
$2p2p\ ^1S^e$	$[2(-1,0)^{+}2]\ ^1S^e$	−1.210(2.4)	−1.154(6.9)	−1.240	−1.244
$2s2p\ ^1P^o$	$[2(0,1)^{+}2]\ ^1P^o$	−1.389(0.2)	−1.336(3.6)	−1.386	−1.386
$2p2p\ ^1D^e$	$[2(1,0)^{+}2]\ ^1D^e$	−1.399(0.4)	−1.350(3.8)	−1.404	
$1s3p\ ^1P^o$	$[1(0,0)^{0}3]\ ^1P^o$	−4.108			
$(2s3p+3s2p)\ ^1P^o$	$[2(0,1)^{+}3]\ ^1P^o$	−1.123			
$(2s3p-3s2p)\ ^1P^o$	$[2(1,0)^{-}3]\ ^1P^o$	−1.187			
$2p3d\ ^1P^o$	$[2(-1,0)^{0}3]\ ^1P^o$	−1.090			

Here $r_{pk}(k=1,2)$ represent distances between the kth electron and the projectile, and Z_p is the charge of the bare projectile ion. To compute this integral stably, we transform r_{pk} into the integral expression in the momentum space ($\mathbf{Q}$). Then we have

$$\left\langle j\left|\frac{1}{r_{pk}}\right|i\right\rangle=\frac{1}{2\pi^2}\int\frac{\langle j|e^{i\mathbf{Q}\cdot(\mathbf{R}-\mathbf{r}_k)}|i\rangle}{Q^2}d\mathbf{Q}\ . \tag{4}$$

Here $\mathbf{R}$ is the internuclear distance between A^{Z_p+} and He, and $\mathbf{r}_k$ is the radius vector of the kth electron. The transition form factor for the $\langle j|e^{i\mathbf{Q}\cdot\mathbf{r}_k}|i\rangle$ is rapidly decreasing as Q increases. The integrand of integral (4) shows no strong oscillations. To test accuracy of the evaluation of the integrals, we have made a pilot calculation taking $Q_{\max}=20$ and 30 a.u. as the upper limit of the Q integration. The difference is found to be less than 0.2%. Hence we fix $Q_{\max}$ of the Q integration at 30 a.u. throughout the calculation. Finally to test our computer code, we have confirmed that calculated cross sections from the ground state to the four singly excited states ($1s2s\ ^1S^e$, $1s2p\ ^1P^o$, $1s3p\ ^1P^o$, $1s3d\ ^1D^e$) reproduce those by Flannery [20], Hippler and Schartner [21], and van den Bos [22] reasonably.

C. Classification of doubly excited states

In addition to the labeling of the doubly excited states based on the conventional independent particle model, we employ the classification scheme of the doubly excited states proposed by Lin [23] in later discussion. This classification scheme is expressed by the set of the quantum numbers $[N(K,T)^A n]^{2S+1}L^\pi$. Here $N(n)$ is the principal quantum number of the inner (outer) electron, and K, T, and A are the so-called correlation quantum numbers and their definitions are given below. Other quantum numbers L, S, and π are defined as usual.

The quantum number K is proportional to $-\langle r_< \cos\theta_{12}\rangle$, while T^2 is proportional to $\langle(\mathbf{L}\hat{\mathbf{r}}_>)^2\rangle$, and the quantum number T expresses the projection of the total angular momentum L onto the mean molecular axis. Here $\mathbf{r}_{<(>)}$ is the radius vector of the inner (outer) electron and θ_{12} is an angle between the radius vectors of the two electrons. These quantum numbers take the following values:

$$T=0,1,\ldots,\min(L,N-1)\ , \tag{5}$$

$$K=N-T-1,N-T-3,\ldots,-(N-T-1)\ . \tag{6}$$

The quantum number A describes the radial correlation of the two atomic electrons. This quantum number is set equal to $+(-)$ if the angular channel function has antinode (node) at $\alpha=\pi/4$ where α is a hyperangle defined by $\alpha=\tan^{-1}(r_2/r_1)$. Other channels are assigned to $A=0$ where their channel functions do not have substantial amplitude around $\alpha=\pi/4$ for almost all hyperradius $R\,[=(r_1^2+r_2^2)^{1/2}]$ but reside away at $\alpha=0$ or $\pi/2$. Hence the states with $A=0$ show weak radial correlation and are considered to be singly excited. According to the rovibrator model [24–26], the He atom in the doubly excited states behaves like a floppy linear triatomic "e-He^{2+}-e" molecule. Then the quantum number $v\,(=N-K-1)$ can be interpreted as the quantum number of the doubly degenerate bending vibrational modes of the floppy "e-He^{2+}-e" linear triatomic molecule, while T is the vibrational angular momentum around the mean molecular axis. For later discussion, the second column of Table I lists the labelings based on this classification scheme corresponding to those of the conventional independent particle model in the first column.

III. RESULTS AND DISCUSSION

A. Total cross sections

We expand the total wave function in terms of 15, 21, and 27 states. Then we calculate three sets of the excitation cross section to the doubly excited states by the proton and C^{6+} ion impact at 1.5 MeV/u impact energy using the close-coupling method. Our calculated results are given in Tables II(a) and II(b). The 15 states included in the close-coupling (CC) calculation are $1s1s\ ^1S^e$, $1s2s\ ^1S^e$, $1s2p\ ^1P^o$, $2s2s\ ^1S^e$, $2p2p\ ^1S^e$, $2s2p\ ^1P^o$, and $2p2p\ ^1D^e$ states. In the CC calculation with the 21 states included, we add the $1s3p\ ^1P^o$, and $(2s3p+3s2p)\ ^1P^o$ states to the set of 15 states mentioned above. Further in the 27-state calculation, we add the $(2s3p-3s2p)\ ^1P^o$ and $2p3d\ ^1P^o$ states to the set of the 21 states given above. For the proton impact [see Table II(a)], we have found that the CC results with the 21 states agree very well with those with the 27 states and converge at least within our choice of the states included. However, for the C^{6+}-ion impact [see Table II(b)], the CC calculation with the 21 states appears to show somewhat slower convergence for the $2p2p\ ^1S^e$ and $2p2p\ ^1D^e$ states at 1.5 MeV/u. This arises from the fact that the couplings among the doubly excited states become stronger as the charge of the projectile is higher. Therefore in the present paper we will discuss the proton and antiproton collisions using the CC results with the 21 states, while for the C^{6+}-ion impact, we employ the CC results with the 27 states, though the convergence is not fully confirmed.

TABLE II. Comparison among three sets of cross sections (in units of 10^{-20} cm^2) for each double excitation process at impact energy of 1.5 MeV/u. Three sets of cross sections are calculated with different size of the expansion, i.e., 15, 21, and 27 states.

Final state	15	21	27
	(a) Proton impact		
$2s2s\ ^1S^e$	0.408	0.409	0.410
$2s2p\ ^1P^o$	7.72	7.74	7.74
$2p2p\ ^1S^e$	0.128	0.116	0.115
$2p2p\ ^1D^e$	0.164	0.191	0.191
	(b) C^{6+}-ion impact		
$2s2s\ ^1S^e$	67.7	71.9	71.6
$2s2p\ ^1P^o$	129.2	131.0	131.0
$2p2p\ ^1S^e$	19.0	11.3	9.88
$2p2p\ ^1D^e$	176.6	211.9	207.5

For the proton, antiproton, and C^{6+}-ion impact at 1.5 MeV/u, Table III compares our calculated results of the CC and the second-order Born calculations with the other experimental data of Giese *et al.* [7] and theoretical results of Fritsch and Lin [9]. Note that the present cross sections are those of the 21-state CC calculation. In the second-order Born calculations, we include the 15 states listed above as intermediate ones. Here the experimental data by electron impact at the corresponding velocity [7] are given in Table III(b) because the data by the antiproton impact are not available at present. For the proton and antiproton impact, our CC results are not in such good agreement with the others for the processes to all the doubly excited states. On the other hand, for the C^{6+}-ion impact, our CC results are in qualitative agreement with those by Fritsch and Lin except for the $2p2p\ ^1S^e$ state, but do not agree with those by Giese *et al.* The discrepancy between our results and those of Fritsch and Lin [9] mainly comes from the different types of wave functions employed in the close-coupling calculation. Fritsch and Lin used the configuration interaction (CI) to take account of the electron-electron correlation. The CI wave functions employed in Ref. [9] include four main doubly excited electron configurations in addition to $1s^2$, $1s2s$, and $1s2p$ configurations with the effective charges optimized [10]. On the other hand, we employ the hyperspherical-coordinate approach [16–18] to generate our wave functions. These wave functions are constructed based on the adiabatic approximation in a hyperspherical coordinate's sense, namely, are written as the product of hyperradial functions and channel functions. Our $^1S^e$, $^1P^o$, and $^1D^e$ channel functions are expanded in terms of 25, 35, and 47 basis functions, respectively. Table I enables us to assess the quality of the wave functions employed in our calculations and in Ref. [9] [compare entries of column (3) with those of column (4) of Table I]. Hence we consider that our hyperspherical wave functions are more flexible and reliable for the description of the electron-electron correlation. It should be noted that the calculated matrix elements of physical quantities other than energy are quite sensitive to the quality of the wave functions employed in comparison with the case of the binding energy. This may explain the differences between our double-electron-excitation cross sections and those presented in Ref. [9].

Table III shows that the second-order Born approximation can reproduce the close-coupling-type calculation of the proton and the antiproton impact qualitatively. This implies that nth higher-order processes with $n > 2$ do not give a significant contribution to double-electron excitation in the proton and antiproton impact at 1.5 MeV/u. However, it fails to give a reasonable description of the excitation by the C^{6+} ion impact at 1.5 MeV/u. This failure is attributable to the fact that the perturbative approach is no longer valid for the C^{6+} impact at 1.5 MeV/u because of the strong interaction with the higher Z_p. There is some difficulty in the procedure of extracting the experimental "total double excitation cross sections" from the ejected electron spectra. In the analysis of the ejected electron spectra, one usually uses the Fano profile with Shore's parametrization. However, one cannot extract the double-electron-excitation cross sections from the parameters of Shore's formula fitted to the ejected electron spectra because of the interference between the direct ionization and the double-electron excitation [9,27]. With this in mind, we consider that the comparison between experiment and theory presented in Table III is still preliminary.

Table IV shows the double-electron-excitation cross sections at 1.5 and 8 MeV/u by the proton and antipro-

TABLE III. Comparison with other experimental and theoretical results of cross sections (in units of 10^{-20} cm^2) for each double-excitation process at impact energy of 1.5 MeV/u. The first column lists final states, the second and third columns give our close-coupling and second-order Born results. The fourth column shows the experimental data by Giese *et al.* [7]. The entries in (b) are the experimental data by electron impact at the same velocity [7] instead of those by the antiproton impact. The fifth column lists the theoretical cross sections given by Fritsch and Lin [9].

Final state	Close coupling	Second-order Born	Giese *et al.* [7]	Fritsch and Lin [9]
		(a) Proton impact		
$2s2s\ ^1S^e$	0.409	0.622	0.0318	0.74
$2s2p\ ^1P^o$	7.74	8.72	0.608	3.0
$2p2p\ ^1S^e$	0.116	0.168		0.45
$2p2p\ ^1D^e$	0.191	0.164	1.84	0.48
		(b) Antiproton impact		
$2s2s\ ^1S^e$	0.314	0.538	0.0816	0.73
$2s2p\ ^1P^o$	7.65	8.61	1.17	3.3
$2p2p\ ^1S^e$	0.0981	0.145		0.41
$2p2p\ ^1D^e$	0.185	0.174		0.27
		(c) C^{6+}-ion impact		
$2s2s\ ^1S^e$	71.6	346	10.9	51.6
$2s2p\ ^1P^o$	131.0	1130	31.1	162
$2p2p\ ^1S^e$	9.88	112		48.6
$2p2p\ ^1D^e$	207.5	197	170	156

ton impact calculated by the close-coupling method. We also give the cross sections to each doubly excited state evaluated by the first-order Born approximation in the same table. Comparing our calculated cross sections with them, we can assess the importance of the second- and higher-order processes in the double-electron-excitation process. Here it should be noted that "order" of the process is defined with respect to the electron-projectile interactions, i.e., expression (3). There exist several terminologies based on the independent particle model such as "shake-up," "two-step first-order," and so forth which are frequently used in the many-body perturbative approach. However, there is no clear cut way of separating, for example, the so-called shake-up amplitude from our calculated amplitude. Hence in later discussion we will not attempt to interpret our results using the terminologies based on this model. We have found that the first-order process dominates in the excitation process to the $2s2p\ ^1P^o$ state, while in the other excitation processes the first- and second-order processes make comparable contributions at 1.5 MeV/u [compare columns (1) with (2) in Tables IV(a) and IV(b)]. At higher 8 MeV/u the second-order processes make considerable contribution only to the excitation to the $2p2p\ ^1D^e$ state [compare columns (1) with (2) in Tables IV(c) and IV(d)]. We have also assessed the importance of each intermediate state by evaluating a set of the cross sections with a particular state excluded from the 21-state CC calculation.

The difference between the cross section by the proton impact $\sigma(p)$ and that by the antiproton impact $\sigma(\bar{p})$ mainly comes from the interference between the first- and second-order processes. Figure 1 shows the total cross sections from the ground state to the four doubly excited ($2s2s\ ^1S^e$, $2s2p\ ^1P^o$, $2p2p\ ^1D^e$, and $2p2p\ ^1S^e$) states as a function of impact energy by proton and antiproton impact, respectively. From Fig. 1, we find that the difference between $\sigma(p)$ and $\sigma(\bar{p})$ for the double-electron excitation is smaller than that in the case of the double ionization at 1.5 MeV/u (see also Table III). A set of the cross sections to the $2s2s\ ^1S^e$ state for the proton and antiproton collisions shows the largest difference. Namely, for this excitation, $\sigma(p)$ is about 0.409×10^{-20} cm^2, and $\sigma(\bar{p})$ is about 0.314×10^{-20} cm^2 at 1.5 MeV/u. The latter is about 0.8 times as small as the former, while for the double ionization, the latter is twice as large as the former [1]. This is different from the conclusion obtained in Ref. [9] that the largest difference between $\sigma(p)$ and $\sigma(\bar{p})$ is seen for the excitation to the $2p2p\ ^1D^e$ state.

For understanding the mechanism of the excitation process from the ground state to the doubly excited states in ion-atom collisions, it is necessary to investigate the role of the intermediate states in more detail. In order to study what states is important as an intermediate one, we truncate one particular state from the set of 21 states, and calculate the excitation cross section to each doubly excited state [see columns (3)–(5) in Table IV]. Then we

TABLE IV. Double-electron-excitation cross sections (in units of 10^{-20} cm^2) of He atoms at 1.5 and 8 MeV/u impact energies by proton and antiproton impact. Column (1) lists sets of the cross sections calculated with the 21 states by the close-coupling method, column (2) gives those by the first-order Born approximation, and columns (3)–(5) give the calculated cross sections with the following state excluded from the set of 21 states: (3), $1s2s\ ^1S^e$; (4), $1s2p\ ^1P^o$; (5), $2s2p\ ^1P^o$. The entries given in parentheses of column (5) of (a) are the calculated cross sections with the $2s2p\ ^1P^o(M=0)$ state only excluded from the set of the 21 states.

Final states	(1)	(2)	(3)	(4)	(5)
		(a) Proton impact at 1.5 MeV/u			
$2s2s\ ^1S^e$	0.409	0.329	0.415	0.405	0.331(0.344)
$2s2p\ ^1P^o$	7.74	8.03	7.92	7.75	
$2p2p\ ^1S^e$	0.116	0.074 0	0.119	0.103	0.067 3(0.0891)
$2p2p\ ^1D^e$	0.191	0.016 8	0.195	0.052 5	0.118
		(b) Antiproton impact at 1.5 MeV/u			
$2s2s\ ^1S^e$	0.314	0.329	0.315	0.320	0.334
$2s2p\ ^1P^o$	7.65	8.03	7.59	7.74	
$2p2p\ ^1S^e$	0.098 3	0.074 0	0.099 6	0.073 6	0.080 5
$2p2p\ ^1D^e$	0.185	0.016 8	0.182	0.067 3	0.095 4
		(c) Proton impact at 8 MeV/u			
$2s2s\ ^1S^e$	0.064 6	0.061 7	0.064 9	0.064 8	0.061 9
$2s2p\ ^1P^o$	2.11	2.15	2.12	2.11	
$2p2p\ ^1S^e$	0.016 2	0.013 9	0.016 3	0.015 1	0.013 8
$2p2p\ ^1D^e$	0.009 67	0.003 15	0.009 70	0.004 49	0.006 52
		(d) Antiproton impact at 8 MeV/u			
$2s2s\ ^1S^e$	0.061 0	0.061 7	0.061 1	0.061 4	0.062 0
$2s2p\ ^1P^o$	2.08	2.15	2.08	2.09	
$2p2p\ ^1S^e$	0.015 3	0.013 9	0.015 4	0.013 9	0.014 2
$2p2p\ ^1D^e$	0.009 67	0.003 15	0.009 61	0.005 02	0.005 99

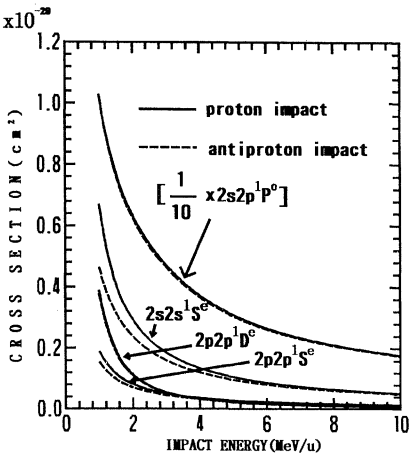

FIG. 1. Energy dependence of the double-electron-excitation cross sections of He atoms by proton impact (solid line) and by antiproton impact (dashed line). The final doubly excited states are the $2s2s\ ^1S^e$, $2s2p\ ^1P^o$, $2p2p\ ^1S^e$, and $2p2p\ ^1D^e$ ones. The cross sections are given in units of 10^{-20} cm^2 for the processes to the $2s2s\ ^1S^e$, $2p2p\ ^1S^e$, and $2p2p\ ^1D^e$ states, and in units of 10^{-19} cm^2 for the process to the $2s2p\ ^1P^o$ state.

compare this cross section with that calculated with the 21 states. When the difference between these two cross sections is large, we identify the state excluded as an important intermediate state. Fritsch and Lin [9] considered the two singly excited $1s2s\ ^1S^e$ and $1s2p\ ^1P^o$ states as intermediate ones. After several test calculations with or without these intermediate states, they concluded that these singly excited states are considered unimportant in the excitation to the doubly excited $^1S^e$ states. We also calculate the excitation cross sections with the two singly excited states excluded from the 21 states. As a result, we have arrived at results similar to Fritsch and Lin's [compare column (1) with (3) and (4) in Table IV(a)]. However, we have also found that the doubly excited $2s2p\ ^1P^o$ state is an important intermediate state in the second-order mechanisms [compare column (1) with (5) in Tables IV(a) and IV(b)]. Namely, we have found that in the excitation processes to the $^1S^e$ states there exist not only the first-order but also the second-order mechanisms. It should be noted that the independent particle model cannot describe this type of second-order mechanism via the doubly excited state.

For excitation to the $2s2s\ ^1S^e$ state, one finds that an important intermediate state for the proton impact is the $2s2p\ ^1P^o$ state. Further we find that the $2s2p\ ^1P^o(M=0)$ (the magnetic quantum number $M=0$) state plays the most significant roles as the intermediate state [see the entries in the parentheses of column (5) in Table IV(a)]. While this process by the antiproton impact seems to be dominated by the first order only [see column (5) in Table IV(b)], the $2s2p\ ^1P^o$ state still plays a significant role as the intermediate state, as we will discuss later. The contribution from the second-order process to this excitation process is not so large, i.e., about 20% for the proton impact at 1.5 MeV/u.

One sees from Table IV that an important intermediate state to the excitation to the $2p2p\ ^1S^e$ state is also the $2s2p\ ^1P^o$ state for the proton and antiproton impact. The contribution from the second-order process is about 40% by the proton impact at 1.5 MeV/u.

As intermediate states to the $2p2p\ ^1D^e$ excitation, one identifies the $1s2p\ ^1P^o$ and $2s2p\ ^1P^o$ states for the proton and antiproton impact. In this case the $1s2p\ ^1P^o$ state plays a more important role as an intermediate state than the $2s2p\ ^1P^o$ state for the proton and antiproton impact. The contribution from the second-order process to the $2p2p\ ^1D^e$ excitation is more than 90% and shows no difference for the proton and antiproton impacts at 1.5 MeV/u as is expected. As the incident energy increases, Tables IV(c) and IV(d) show that the first-order mechanism dominates except for the $2p2p\ ^1D^e$ excitation where the second-order mechanism is essential. Generally speaking, dipole transitions with $\Delta L=1$ are quite likely to take place. Here, there exists the first-order process from the ground state to the doubly excited $2s2p\ ^1P^o$ state with $\Delta L=1$, $\Delta A=0$, $\Delta v=1$, and $\Delta T=1$. This is consistent with the propensity rule previously found for the optically allowed transitions [12,14]. Specifically the $2s2p\ ^1P^o$ doubly excited state plays the important role as the intermediate state in the second-order mechanism of the excitation processes to the doubly excited $^1S^e$ and $^1D^e$ states.

B. Impact-parameter dependence

Figures 2(a) and 2(b) display impact-parameter weighted probabilities from the ground state to the doubly excited $2s2s\ ^1S^e$ state as a function of impact parameter b at 1.5 MeV/u by the proton and antiproton impacts, respectively. There exist two peaks in the b dependence of probability, one at b equal to 0.2 a.u. and the other at 2 a.u., and a dip is seen at $b=1$ a.u. In the excitation process to the $2s2s\ ^1S^e$ state by the antiproton impact, we find that the probability calculated with the $2s2p\ ^1P^o$ state excluded is larger than that with all 21 states included when $b\leq 1$ a.u., while the tendency becomes opposite when $b\geq 1$. As a result, the $2s2p\ ^1P^o$ state dose not apparently influence the total cross section strongly because the integral over b turns out to be nearly equal to that with the $2s2p\ ^1P^o$ state included because of balance of increase and decrease at different impact-parameter regions. Therefore this does not mean that the excitation process is dominated by the first-order process only. On the other hand, for the proton impact, one finds explicit contribution from the second-order mechanism.

For the probabilities to the $2p2p\ ^1S^e$ state compared using the set with the $2s2p\ ^1P^o$ state excluded from a set of the 21 states, we find the same trends as are seen in the case of the process to the $2s2s\ ^1S^e$ state, except that the total cross section becomes smaller.

Figure 3 shows the impact-parameter dependence of the weighted probabilities of the $2s2p\ ^1P^o$ excitation. We also give each component of the probabilities to the magnetic quantum numbers $M=0,\pm 1$ with respect to the space-fixed z axis where the z axis is taken as an incident direction of the projectile. One sees that the total proba-

bility has a maximum around $b \simeq 1$ a.u. According to the classification scheme based on the set of correlation quantum numbers, the $2s2p\ ^1P^o$ state has $K=0$, $T=1$, and $A=+$ as shown in Table I. In this state, the doubly excited He atom as a floppy "e-He^{2+}-e" linear triatomic molecule rotates around the mean molecular axis and is vibrationally excited in the bending vibrational mode (i.e, $v=N-K-1=1$). If one views from the space-fixed frames [28], it is most probable that for $M=\pm 1$, the mean rotation axis of the "e-He^{2+}-e" molecule coincides with the z axis as shown in Fig. 4(a), while for $M=0$, the mean rotation axis becomes perpendicular to the space-fixed quantization z axis as shown in Fig. 4(b). Figure 3 shows that, at $b \simeq 1$ a.u., excitation to the components with $M=\pm 1$ is more likely to take place. The total cross section of the $2s2p\ ^1P^o$ excitation is governed by the

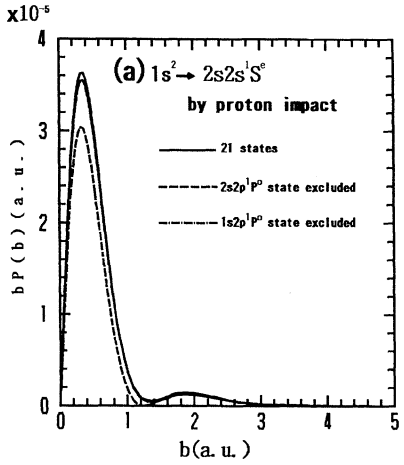

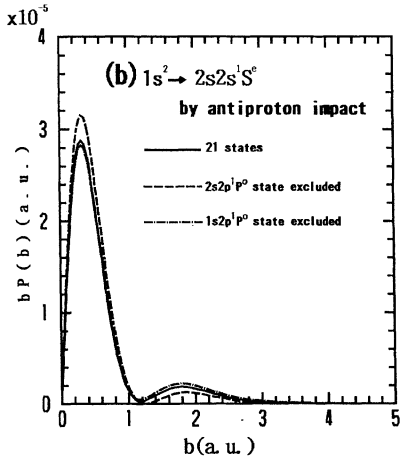

FIG. 2. Impact-parameter weighted probabilities from the ground state to the doubly excited $2s2s\ ^1S^e$ state of He atoms, as a function of impact parameter b at 1.5 MeV/u impact energy: (a) by proton impact, (b) by antiproton impact. The calculations are carried out with a set of the following states: the 21 states (solid line), the $2s2p\ ^1P^o$ state excluded from the 21 states (dashed line), and the $1s2p\ ^1P^o$ state excluded (dash-dotted line).

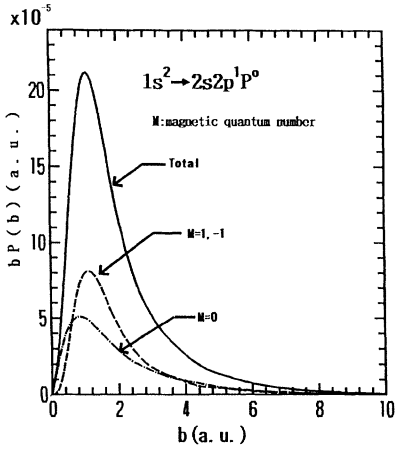

FIG. 3. Impact-parameter weighted probabilities from the ground state to the doubly excited $2s2p\ ^1P^o$ state of He atoms, as a function of impact parameter b at 1.5 MeV/u impact energy: the total probability (solid line), the probabilities to the $2s2p\ ^1P^o(M=\pm 1)$ states (dashed line), and to the $2s2p\ ^1P^o(M=0)$ one (dash-dotted line).

first-order mechanism at large impact parameters b larger than about 1 a.u. in which the doubly excited atom as a floppy linear triatomic molecule is rotationally excited around the mean molecular axis parallel to the space-fixed z axis and is vibrationally excited in the bending vibrational mode.

However, the $2s2p\ ^1P^o(M=0)$ state is a main contributor to the second-order mechanism at small impact pa-

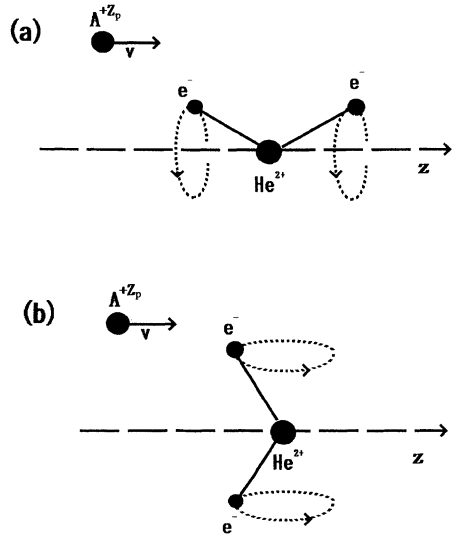

FIG. 4. Correlated motion of the two atomic electrons of the He atom based on the rovibrator model in the $2(0,1)^+2\ ^1P^o$ ($2s2p\ ^1P^o$) state. The z axis is taken as the incident direction of the projectile: (a) Magnetic quantum number $M=1$ (in the case of $M=-1$, the two atomic electrons rotate in the opposite direction around the mean molecular axis), (b) $M=0$.

rameter $b \sim 0.2$ a.u. as mentioned previously. Therefore one can easily visualize how the correlated two atomic electrons behave during the excitation process, i.e., via the $2s2p\ ^1P^o(M=0)$ $[2(0,1)^+2\ ^1P^o(M=0)]$ state [see fig. 4(b)] and is hyper-radially or vibrationally excited in the final state, i.e., attains the radial stretching in the $2s2s\ ^1S^e$ $[2(1,0)^+2\ ^1S^e]$ state or the vibrational excitation of the bending mode in the $2p2p\ ^1S^e$ $[2(-1,0)^+2\ ^1S^e]$ state where $v\,(=N-K-1)$ is 2.

We have found that the impact-parameter dependence of the $2p2p\ ^1D^e$ $[2(1,0)^+2\ ^1D^e]$ state shows the broad peak around large impact parameters $b \simeq 2$ a.u. (not shown here). Table III indicates close agreement with the second-order Born cross section to the $2p2p\ ^1D^e$ state with those of the CC calculation where the perturbative approach is valid at large impact parameters. In this excitation process, the second-order mechanism dominates as we have already seen. We have two important intermediate states, i.e., the $1s2p\ ^1P^o$ $[1(0,0)^02\ ^1P^o]$ state and $2s2p\ ^1P^o$ $[2(0,1)^+2\ ^1P^o]$ state. The former shows weaker correlated motion of two atomic electrons because $A=0$, though it makes a more important contribution to this excitation process. For the second-order process to the $2p2p\ ^1D^e$ $[2(1,0)^+2\ ^1D^e]$ state via the latter $2s2p\ ^1P^o$ $[2(0,1)^+2\ ^1P^o]$ state, we can illustrate the behaviors of the correlated motion of two atomic electrons based on the rovibrator model during the collision process as follows. The He atom as the floppy "e-He^{2+}-e" linear triatomic molecule is vibrationally excited in the bending vibrational mode and is rotationally excited around the mean molecular axis (i.e., $v=T=1$) in the intermediate state. Then eventually in the final $2p2p\ ^1D^e$ $[2(1,0)^+2\ ^1D^e]$ state from the intermediate state, the He atom becomes vibrationally deexcited in the bending vibrational mode, i.e., $\Delta v=-1$ and rotationally further excited $\Delta L=1$. However, the rotation axis becomes perpendicular to the mean molecular axis, i.e., $L=2$ and $T=0$. Eventually from the initial $1s1s\ ^1S^e$ $[1(0,0)^+1\ ^1S^e]$ state with $v=T=0$ to the final $2p2p\ ^1D^e$ $[2(1,0)^+2\ ^1D^e]$ state, the He atom stretches its size conserving internal state (i.e. $\Delta v=\Delta T=0$) and is rotationally excited around the axis perpendicular to the mean molecular axis. However, for the excitation to the $2p2p\ ^1D^e$ state, we have not yet fully elucidated the behaviors of the He atom as the floppy linear triatomic molecule viewed from the space-fixed frame, which we plan to study for a future publication.

C. Time dependence

Finally, we briefly discuss the time evolution of the transition probability during the collision process. Figure 5 shows time dependence of the excitation probabilities to the doubly excited $2s2s\ ^1S^e$ $[2(1,0)^+2\ ^1S^e]$, $2p2p\ ^1S^e$ $[2(-1,0)^+2\ ^1S^e]$, and $2s2p\ ^1P^o$ $[2(0,1)^+2\ ^1P^o]$ $(M=0,\pm1)$ states by the proton and antiproton impact at $b=0.2$ a.u. Here one sees sharp peaks at $t \simeq 0$ for the excitation to $2s2p\ ^1P^o$ $[2(0,1)^+2\ ^1P^o]$ $(M=0)$ state. However, these peaks can be reproduced if we retain only the four states, i.e., $1s1s\ ^1S^e$ $[1(0,0)^+1\ ^1S^e]$ and $2s2p\ ^1P^o$ $[2(0,1)^+2\ ^1P^o]$ in the close-coupling calculation. Therefore these peaks do not contribute to the second-order mechanism of the excitation to the $2s2s\ ^1S^e$ $[2(1,0)^+2^1S^e]$, $2p2p\ ^1S^e[2(-1,0)^+2\ ^1S^e]$ states, and so forth. These behaviors can be easily understood from the angular dependence of the matrix element of the interaction potential, i.e.,

$$V_{ij}(\mathbf{R})=\sum_{l=|L_i-L_f|}^{L_i+L_f} V_{ij}^{lm}(R)Y_{lm}(\theta,\phi) \tag{7}$$

where $V_{ij}(\mathbf{R})=\langle j|V(\mathbf{R})|i\rangle$. Here, Y_{lm} are spherical harmonics and polar angles (θ,ϕ) are defined with respect to the space-fixed z axis, and L_i (L_f) is an angular momentum quantum number of initial (final) state. The value of m equal to M_i-M_f, and M_i (M_f) is a magnetic quantum number of the initial (final) state. For the process from the $^1S^e$ state to the $^1P^o$ state or from the $^1P^o$ state to the $^1S^e$ state, the value of l becomes 1. For the excitation to $M_f=m=0$ component, $V_{ij}(\mathbf{R})$ behaves proportionally to

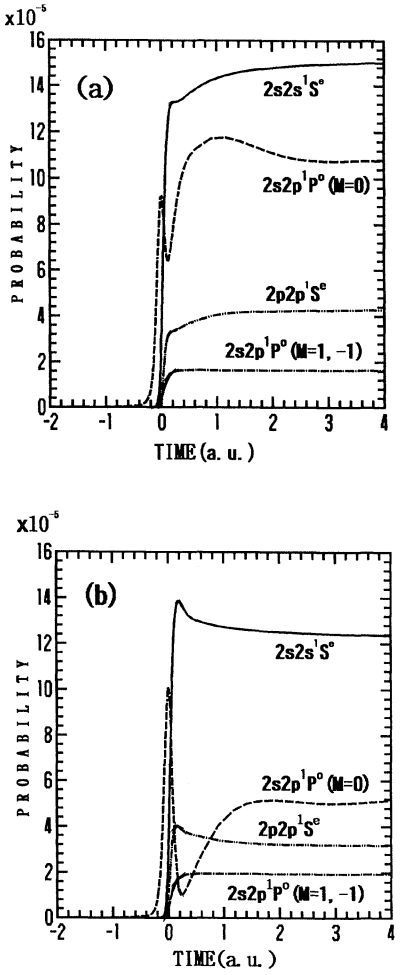

FIG. 5. Time dependence of the excitation probabilities from the ground state to the doubly excited states at the impact parameter of 0.2 a.u.: (a) proton impact, (b) antiproton impact: $2s2s\ ^1S^e$ (solid line), $2s2p\ ^1P^o(M=0)$ (dashed line), $2s2p\ ^1P^o(M=\pm1)$ (dashed-dotted line), and $2p2p\ ^1S^e$ (dashed-dot-dotted line).

$\cos\theta$ because $Y_{10} \propto \cos\theta$. This dependence gives rise to the sharp peak at $t=0$ a.u.

For $t=0\approx 1$ a.u., the excitation probability to the $2s2p\ ^1P^o$ $[2(0,1)^+2\ ^1P^o]$ $(M=0)$ state for the proton impact indicated in Fig. 5(a) shows a more rapid increase than that for the antiproton impact as shown in Fig. 5(b). This difference is considered to arise from the interference effect of the first-order amplitudes with the second-order ones at small impact parameters and causes the different behaviors of the transition probabilities to the $2s2s\ ^1S^e$ $[2(1,0)^+2\ ^1S^e]$ and $2p2p\ ^1S^e$ $[2(-1,0)^+2\ ^1S^e]$ states between the proton and antiproton collisions as shown in Fig. 5.

On the other hand, for the excitation to the doubly excited $2s2p\ ^1P^o$ $[2(0,1)^+2\ ^1P^o]$ $(M_f=\pm 1)$ state, $V_{ij}(\mathbf{R})$ behaves proportionally to $\sin\theta$, and the value of $V_{ij}(\mathbf{R})$ is quite small except for $t\simeq 0$ a.u. at small impact parameters. Therefore the excitation probability to the doubly excited $2s2p\ ^1P^o$ $(M=\pm 1)$ states increases sharply around $t\simeq 0$ a.u., and then, the probabilities for the processes to those states remain constant at later times. This probability is much smaller than that for the process to the doubly excited $2s2p\ ^1P^o$ $(M=0)$ state at this small impact parameter. However, at larger impact parameters, i.e., $b\simeq 1$ a.u., this probability becomes larger, and makes an essential contribution to the total cross section of the $2s2p\ ^1P^o$ state (see also Fig. 3). Therefore the first-order process dominates in the excitation process to the doubly excited $2s2p\ ^1P^o$ state.

IV. SUMMARY AND CONCLUSIONS

We have theoretically investigated the double-electron excitation of He by fast-ion impact using the hyperspherical wave functions for the description of the electron-electron correlation. At 1.5 MeV/u, the first-order processes dominate in the excitation process to the $2s2p\ ^1P^o$ state by the proton and antiproton impact. In the excitation to the $2s2s\ ^1S^e$ and $2p2p\ ^1S^e$ states, the first- and second-order processes give comparable contribution to these processes. In the excitation process to the $2p2p\ ^1D^e$ state, the second-order process dominates. In these processes, the doubly excited $2s2p\ ^1P^o$ state plays an essential role as an intermediate state. As the incident energy increases, say at 8 MeV/u, the first-order processes dominate except for the excitation to the $2p2p\ ^1D^e$ state. We have found that the difference for the double-electron-excitation processes by the proton and antiproton impact is much smaller than that corresponding to the double-ionization processes. We have also shown that interpretation of our calculated results based on the classification scheme of the correlation quantum numbers and on the rovibrator model gives more direct physical insight to the correlated motion of two atomic electrons during the collision processes. We have made a preliminary discussion of our calculated results by the C^{6+}-ion impact because the convergence of the calculated cross sections on the numbers of states included in the close-coupling calculation is less satisfactory compared to that for the proton impact.

ACKNOWLEDGMENTS

We wish to thank S. Watanabe and N. Koyama for their useful discussion. Two of us (M.M. and M.K.) gratefully acknowledge support from the international cooperative research program between the National Science Foundation and the Japan Society for the Promotion of Science. One of us (M.K.) also acknowledges support from the U.S. DOE Office of Health and Environment Research under Contract No. W31-109-Eng-38. Numerical computations were carried out in part at the Computer Center, Institute for Molecular Science, Okazaki National Research Institutes.

[1] L. H. Andersen, P. Hvelplund, H. Knudsen, S. P. Møller, K. Elsener, K. -G. Rensfelt, and E. Uggerhøj, Phys. Rev. Lett. **57**, 2147 (1986).
[2] J. F. Reading and A. L. Ford, Phys. Rev. Lett. **58**, 543 (1987); J. Phys. B **20**, 3747 (1987).
[3] A. L. Ford and J. F. Reading, J. Phys. B **21**, L685 (1988).
[4] J. H. McGuire, Phys. Rev. Lett. **49**, 1153 (1982).
[5] J. H. McGuire, Phys. Rev. A **36**, 1114 (1987).
[6] R. E. Olson, Phys. Rev. A **36**, 1519 (1987).
[7] J. P. Giese, M. Schulz, J. K. Swenson, M. Benhenni, S. L. Varghese, C. R. Vane, P. F. Dittner, S. M. Shafroth, and S. Datz, Phys. Rev. A **42**, 1231 (1990).
[8] J. O. P. Pedersen and P. Hvelplund, Phys. Rev. Lett. **62**, 2373 (1989).
[9] W. Fritsch and C. D. Lin, Phys. Rev. A **41**, 4776 (1990).
[10] W. Fritsch and C. D. Lin, Phys. Rev. Lett. **61**, 690 (1988).
[11] M. Matsuzawa, T. Motoyama, H. Fukuda, and N. Koyama, Phys. Rev. A **34**, 1793 (1986).
[12] T. Motoyama, N. Koyama, and M. Matsuzawa, Phys. Rev. A **38**, 670 (1988).
[13] M. Matsuzawa, T. Atsumi, and N. Koyama, Phys. Rev. A **41**, 3596 (1990).
[14] T. Atsumi, T. Ishihara, N. Koyama, and M. Matsuzawa, Phys. Rev. A **42**, 6391 (1990).
[15] P. G. Burke, Adv. At. Mol. Phys. **4**, 173 (1968).
[16] N. Koyama, H. Fukuda, T. Motoyama, and M. Matsuzawa, J. Phys. B **19**, L331 (1986).
[17] H. Fukuda, N. Koyama, and M. Matsuzawa, J. Phys. B **20**, 2959 (1987).
[18] N. Koyama, A. Takafuji, and M. Matsuzawa, J. Phys. B **22**, 553 (1989).
[19] Y. K. Ho, Phys. Rev. A **23**, 2137 (1981).
[20] M. R. Flannery, J. Phys. B **3**, 306 (1970).
[21] R. H. Hippler and K. -H. Schartner, J. Phys. B **7**, 618 (1974).
[22] J. van den Bos, Phys. Rev. **181**, 191 (1969).
[23] C. D. Lin, Phys. Rev. A **29**, 1019 (1984).
[24] C. D. Lin, Adv. Mol. Phys. **22**, 77 (1986).
[25] D. R. Herrick and M. E. Kellman, Phys. Rev. A **21**, 418 (1980).
[26] M. E. Kellman and D. R. Herrick, Phys. Rev. A **22**, 1536 (1980).
[27] V. V. Balashov, S. S. Lipovetskiĭ, and V. S. Senashenko, Zh. Eksp. Teor. Fiz. **63**, 1622 (1972) [Sov. Phys.—JETP **36**, 858 (1973)].
[28] S. Watanabe and C. D. Lin, Phys. Rev. A **34**, 823 (1986).